Formation and Antitumor Activity of PNU-159682, A Major Metabolite of Nemorubicin in Human Liver Microsomes

Luigi Quintieri,[1,2] Cristina Geroni,[3] Marianna Fantin,[1] Rosangela Battaglia,[3] Antonio Rosato,[2] William Speed,[4] Paola Zanovello,[2] and Maura Floreani[1]

[1]Department of Pharmacology and Anesthesiology, Pharmacology Section and [2]Department of Oncology and Surgical Sciences, Oncology Section, University of Padua, Padua, Italy; [3]Nerviano Medical Science S.r.l., Nerviano, Italy; and [4]Department of Pharmacokinetics, Dynamics and Metabolism, Pfizer Global Research and Development, Sandwich, Kent, United Kingdom

ABSTRACT

Purpose: **Nemorubicin (3′-deamino-3′-[2″(*S*)-methoxy-4″-morpholinyl]doxorubicin; MMDX) is an investigational drug currently in phase II/III clinical testing in hepatocellular carcinoma. A bioactivation product of MMDX, 3′-deamino-3″,4′-anhydro-[2″(*S*)-methoxy-3″(*R*)-oxy-4″-morpholinyl]doxorubicin (PNU-159682), has been recently identified in an incubate of the drug with NADPH-supplemented rat liver microsomes. The aims of this study were to obtain information about MMDX biotransformation to PNU-159682 in humans, and to explore the antitumor activity of PNU-159682.**

Experimental Design: **Human liver microsomes (HLM) and microsomes from genetically engineered cell lines expressing individual human cytochrome *P*450s (CYP) were used to study MMDX biotransformation. We also examined the cytotoxicity and antitumor activity of PNU-159682 using a panel of *in vitro*-cultured human tumor cell lines and tumor-bearing mice, respectively.**

Results: **HLMs converted MMDX to a major metabolite, whose retention time in liquid chromatography and ion fragmentation in tandem mass spectrometry were identical to those of synthetic PNU-159682. In a bank of HLMs from 10 donors, rates of PNU-159682 formation correlated significantly with three distinct CYP3A-mediated activities. Troleandomycin and ketoconazole, both inhibitors of CYP3A, markedly reduced PNU-159682 formation by HLMs; the reaction was also concentration-dependently inhibited by a monoclonal antibody to CYP3A4/5. Of the 10 cDNA-expressed CYPs examined, only CYP3A4 formed PNU-159682. In addition, PNU-159682 was remarkably more cytotoxic than MMDX and doxorubicin *in vitro*, and was effective in the two *in vivo* tumor models tested, i.e., disseminated murine L1210 leukemia and MX-1 human mammary carcinoma xenografts.**

***Conclusions*: CYP3A4, the major CYP in human liver, converts MMDX to a more cytotoxic metabolite, PNU-159682, which retains antitumor activity *in vivo*.**

INTRODUCTION

The clinical use of classical anthracyclines, such doxorubicin and daunorubicin, is limited by their dose-related cardiotoxicity, myelosuppression, and intrinsic or acquired tumor resistance. Among the several anthracycline analogues synthesized in an effort to obtain less toxic and more effective antitumor agents, nemorubicin (3′-deamino-3′-[2″(*S*)-methoxy-4″-morpholinyl]doxorubicin; MMDX), a doxorubicin derivative bearing a methoxymorpholinyl group at position 3′ of the sugar moiety, has been selected for clinical evaluation. Unlike doxorubicin, MMDX is also highly cytotoxic to a variety of tumor cell lines presenting a multidrug-resistant phenotype both *in vitro* and *in vivo* (1–3), and is not cardiotoxic at therapeutic doses (4); it is presently undergoing a phase II/III clinical trial for intrahepatic artery chemotherapy of hepatocellular carcinoma, with a preliminary response rate of about 25% (5). MMDX is remarkably more potent *in vivo* than currently clinically available anthracyclines, its maximum tolerated dose being 50- to 130-fold lower than that of doxorubicin, in both experimental animals and humans (1, 6). By contrast, MMDX is only 2- to 10-fold more cytotoxic than doxorubicin *in vitro* (4, 7).

Previous *in vitro* studies showed that the cytotoxicity of MMDX is markedly enhanced upon its exposure to NADPH-supplemented liver microsomes from different animal species, including humans, and identified cytochrome *P*450s (CYP) belonging to the 3A subfamily as the enzymes responsible for hepatic bioactivation of the drug (8–10). Further studies in tumor-bearing and healthy mice revealed that a metabolite(s) formed via CYP3A mediates both therapeutic efficacy and host toxicity of MMDX (9).

To date, the only metabolite of MMDX consistently found in the plasma of patients and experimental animals receiving the drug is 13(*S*)-dihydro-MMDX, which is formed via stereoselective reduction of the side chain C_{13}-carbonyl group of MMDX (6, 11). Like most of 13-dihydro metabolites of other anthracyclines (12), 13-dihydro-MMDX shows a lower cytotoxicity than its parent compound *in vitro*.[5] However, the existence in humans of a circulating bioactivation product(s) of MMDX is supported by the finding that plasma samples from drug-treated

Received 9/13/04; revised 11/15/04; accepted 11/24/04.
Grant support: Supported by National Research Council of Italy Grant CNRG00C1F7 (L. Quintieri) and a grant from the Italian Ministry for Education, University and Research (MIUR).
The costs of publication of this article were defrayed in part by the payment of page charges. This article must therefore be hereby marked *advertisement* in accordance with 18 U.S.C. Section 1734 solely to indicate this fact.
Requests for reprints: Luigi Quintieri, Department of Pharmacology and Anesthesiology, University of Padua, Largo Meneghetti 2, I-35131 Padua, Italy. Phone: 39-049-827-5083; Fax: 39-049-827-5093; E-mail: luigi.quintieri@unipd.it.

[5] L. Capolongo, et al. *In vitro* cytotoxicity of anthracycline aglycones and 13-OH derivatives. Pharmacia Internal Report No. 222i, October 1993, unpublished data.

patients are much more cytotoxic to cultured human hemopoietic cells than expected on the basis of their MMDX content (13).

Three oxidative metabolites of MMDX, i.e., MMDX *N*-oxide, 3′-deamino-3′-[2″(*S*)-methoxy-5″-oxo-4″-morpholinyl]-doxorubicin (PNU-159696), and 3′-deamino-3″,4′-anhydro-[2″(*S*)-methoxy-3″(*R*)-oxy-4″-morpholinyl]doxorubicin (PNU-159682), have been recently isolated from an incubate of the drug with NADPH and liver microsomes from dexamethasone-induced male rats (14). Preliminary cytotoxicity experiments using cultured murine L1210 tumor cells as targets revealed that, whereas MMDX *N*-oxide and PNU-159696 possess a potency comparable to that of MMDX, PNU-159682 represents a bioactivation product being more than 3,000-fold more cytotoxic than its parent compound (14). Furthermore, although the low therapeutic dosages of MMDX hinder the detection of this drug and its metabolites in biological fluids and tissues, traces of PNU-159682 have been detected in a plasma sample from a cancer patient receiving prolonged i.v. infusion of MMDX, as well as in the liver extracts of tumor-bearing mice receiving optimal antitumor doses of the drug as i.v. bolus.[6] This study was therefore undertaken to investigate the ability of isolated human liver microsomes (HLM) to catalyze conversion of MMDX to PNU-159682, to identify the enzyme(s) responsible for the reaction, and to further explore the biological activity of PNU-159682, in terms of both *in vitro* tumor cell growth inhibition and *in vivo* therapeutic efficacy.

MATERIALS AND METHODS

Materials

[^{14}C]MMDX (1.79 GBq/mmol; radiochemical purity of 93%), unlabeled MMDX, racemic 13-dihydro-MMDX, doxorubicin (all as hydrochloride salts), MMDX *N*-oxide, and PNU-159682 (as free base), were synthesized at Pharmacia Italia S.p.A. (Nerviano, Italy). Methanol, acetonitrile, ethanol and dichloromethane [all high-performance liquid chromatography (HPLC) grade] were from Carlo Erba Reagenti (Milan, Italy). Oxidized nifedipine [2,6-dimethyl-4-(2′-nitrophenyl)-3,5-pyridinedicarboxylic acid dimethyl ester] was obtained from Ultrafine (UFC, Ltd., Manchester, United Kingdom). Unless indicated otherwise, all other chemicals were purchased from Sigma-Aldrich Co. (St. Louis, MO).

Inhibitory monoclonal antibodies (MAb) to human CYP enzymes were generously donated by Dr. H.V. Gelboin (Laboratory of Molecular Carcinogenesis, National Cancer Institute, NIH, Bethesda, MD). These were: MAbs 26-7-5 (anti-CYP1A2), 49-10-20 (anti-CYP2B6), 281-1-1 (anti-CYP2C8), 763-15-5 (anti-CYP2C9), 1-7-4-8 (anti-CYP2C19), 512-1-8 (anti-CYP2D6), and 3-29-9 (anti-CYP3A4/5; refs. 15–19). Pooled HLMs (mixed gender; $n = 21$) and microsomes prepared from 10 different human livers were provided by BD Gentest (Woburn, MA). Microsomes from cDNA-transfected human B-lymphoblastoid cells expressing CYP1A2, CYP2A6, CYP2B6, CYP2C8, CYP2C9*1, CYP2C19, CYP2D6*1, CYP2E1, CYP3A4, and microsomes from baculovirus-infected insect cells expressing CYP3A5 were also obtained from BD Gentest.

Evaluation of Nifedipine Oxidase and Erythromycin N-Demethylase Activities

Nifedipine oxidase activity of each individual liver microsomal sample was estimated as described by Guengerich et al. (20).

Erythromycin *N*-demethylase activity was determined in incubation mixtures containing 1 mmol/L substrate, 0.25 mg protein/mL of HLMs, and 1 mmol/L NADPH in 0.1 mol/L potassium phosphate buffer (pH 7.4; total volume, 0.4 mL). The reaction was started by the addition of microsomes following a 3-minute preincubation at 37°C, conducted in a shaking water bath at 37°C for 10 minutes, and stopped by the addition of 0.1 mL of ice-cold ethanol. The formaldehyde formed was then determined by a modification of the method of Jones et al. (21). In detail, after protein precipitation, 0.4 mL of clear supernatant was transferred into a tube containing 80 μL of freshly prepared Nash's reagent [15% (w/v) ammonium acetate, 0.3% (v/v) acetic acid, and 0.2% (v/v) 2,4-pentandione in distilled water]. The tubes were capped and placed in a water bath at 51°C for 12 minutes to allow formation of a formaldehyde derivative (3,5-diacetyl-1,4-dihydrolutidine), which was then separated from interferences and quantified by HPLC as described below.

Incubation of MMDX with Human Liver Microsomes

General Incubation Procedure. A typical incubation mixture consisted of 0.3 mol/L Tris (pH 7.4), 0.5 mmol/L NADPH, 0.25 mg protein/mL of HLMs and MMDX or [^{14}C]MMDX (1-50 μmol/L) in a total volume of 0.2 mL. The reactions were started by adding the microsomes following a 3-minute preincubation at 37°C, conducted in a shaking water bath at 37°C under aerobic conditions, and stopped, typically after 10 minutes, by adding 0.2 mL of ice-cold methanol. Control incubations were conducted in the absence of NADPH or using boiled microsomes. After protein precipitation, an aliquot of the supernatant was analyzed by HPLC with fluorescence detection, or combined UV and radiometric detection, or by liquid chromatography with tandem mass spectrometry detection (LC-MS/MS), as described below.

Kinetic Analysis of PNU-159582 Formation. Incubations for analysis of enzyme kinetics were carried out at eight MMDX concentrations ranging from 1 to 50 μmol/L; the incubation protocol was the same as that described above. Enzyme kinetic parameters (K_m and V_{max}) were determined by fitting the reaction velocity versus substrate concentration data to the single enzyme Michaelis-Menten equation using the SigmaPlot 8.0 software (SPSS, Inc., Chicago, IL).

Correlation Studies. MMDX (20 μmol/L) was incubated with microsomal fractions from 10 individual human livers; the incubation protocol was the same as that described above. The rates of PNU-159682 formation obtained in these experiments were correlated with several known CYP form-selective catalytic activities evaluated in the same microsomal samples (data provided by BD Gentest except those for nifedipine oxidation and erythromycin *N*-demethylation). Coefficients of determination (r^2) and *P* values were determined by linear regression

[6] M.A. Pacciarini and C. Geroni, unpublished results.

analysis (GraphPad Instat version 2.02; GraphPad Software, San Diego, CA).

Chemical and Immunochemical Inhibition Studies. Formation of PNU-159682 from 20 μmol/L MMDX by pooled HLMs was evaluated in the absence (i.e., control) and presence of known CYP form-selective chemical inhibitors. The following inhibitors were examined at concentrations previously identified as being appropriate to cause CYP form-selective inhibition in HLMs: 7,8-benzoflavone (1 μmol/L, CYP1A2-selective; refs. 22, 23), sulfaphenazole (20 μmol/L, CYP2C9-selective; ref. 22), quinidine (5 μmol/L, CYP2D6-selective; ref. 22), diethyldithiocarbamate (25 μmol/L; CYP2A6/E1-selective; ref. 24), troleandomycin (100 μmol/L, CYP3A-selective; ref. 22) and ketoconazole (1 μmol/L, CYP3A-selective; ref. 25). In experiments with reversible inhibitors, i.e., 7,8-benzoflavone, quinidine, sulfaphenazole, and ketoconazole, the inhibitor was coincubated with the substrate; the incubation protocol was the same as described above. In experiments with mechanism-based inhibitors, i.e., diethyldithiocarbamate and troleandomycin, the inhibitor was preincubated with liver microsomes and NADPH (0.5 mmol/L) at 37°C for 15 minutes before adding the substrate and additional 0.5 mmol/L NADPH. The reactions were then conducted as described above.

Immunochemical inhibition studies were carried out using mouse ascites fluids containing inhibitory MAbs which have been shown to be specific for different human CYP enzymes (15–19). Pooled HLMs (0.25 mg microsomal protein/mL; 20 pmol of total CYP) were preincubated with the designated amount of mouse ascites containing anti-CYP MAb (20-140 μg) at 37°C for 5 minutes in 0.3 mol/L Tris (pH 7.4); the reaction was then initiated by the addition of MMDX (final concentration, 20 μmol/L) and NADPH (final concentration, 0.5 mmol/L) in a total volume of 0.2 mL, and conducted as described above. The highest concentration of each MAb used in these trials (i.e., 7 μg ascites protein/pmol of total CYP) was previously shown to be saturating for an appropriate CYP form-specific reaction in HLMs (15–19). Control incubations were carried out in the absence of MAb.

Incubation of MMDX with cDNA-expressed Human Cytochrome *P*450 Enzymes

Incubations of MMDX with microsomes containing cDNA-expressed CYP enzymes were done as described for HLMs, except that the amount of enzyme used was 50 pmol/mL and incubations were terminated after 60 minutes; substrate concentration was 20 μmol/L. All incubations were done in duplicate. Aliquots of the supernatants from each sample were analyzed for PNU-159682 content by HPLC with fluorescence detection.

High-Performance Liquid Chromatography Analyses

Radio-High-Performance Liquid Chromatography Analysis. To investigate the overall liver microsomal metabolic profile of MMDX, analysis of incubation mixtures was carried out using an HPLC system consisting of a series 200 LC pump fitted with a solvent degasser (all from Perkin-Elmer Corp., Norwalk, CT), an AS-950 autosampler (Jasco, Inc., Tokyo, Japan), an LC 295 UV-Visible detector (Perkin-Elmer), and a 515TR radioactivity flow detector (Packard Instruments, Meriden, CT) equipped with a 0.5 mL homogeneous flow cell. Chromatographic conditions were as follows: column, Simmetry C_{18} (4.6 × 150 mm, 3.5 μm; Waters Corp., Milford, MA); mobile phase, 10 mmol/L KH_2PO_4 (pH 5.5)/methanol/acetonitrile (45:30:25, v/v/v); flow rate, 1 mL/min; injection volume, 20 to 50 μL; column temperature, ambient; detection, UV absorbance at 254 nm and radioactivity using Ultima-Flo M liquid scintillation cocktail (Packard Instruments) at a 3:1 ratio. Data were collected and processed using the Flo-one software (Packard Instruments).

Structural Identification of PNU-159682 by Liquid Chromatography with Tandem Mass Spectrometry Detection. The chromatographic system consisted of a 2690 Alliance separation module including a gradient HPLC pump, an autosampler and a column oven (Waters), a TSP UV 600 variable-wavelength UV detector (ThermoFinnigan, San Jose, CA) and an LCQ classic ion-trap mass spectrometer (ThermoFinnigan). Chromatographic conditions were as follows: column, Xterra MS C_8 (2.1 × 150 mm, 5 μm; Waters); mobile phase, 10 mmol/L ammonium formate (pH 4.5; solvent A) and acetonitrile (solvent B); elution program, linear gradient from 0% to 70% solvent B from 1 to 10 minutes, followed by isocratic elution with 70% solvent B for an additional 6 minutes; flow rate, 0.3 mL/min; injection volume, 50 μL; column temperature, 40°C; detection, visible absorbance at 490 nm and tandem mass spectrometry. With the above conditions, retention times of MMDX and PNU-159682 were 9.9 and 11.7 minutes, respectively. The mass spectrometer operated under the following conditions: electrospray in positive ion mode; source voltage, 5 kV; capillary voltage, 31 V; capillary temperature, 230°C; tube lens offset, −20 V. Data were collected by full scan mode (scan range of m/z, 175-700) and analyzed by the Xcalibur software package (ThermoFinnigan). Tandem mass spectra were collected using a collision energy of 50% with wideband activation.

Quantitation of PNU-159682. Quantitative evaluation of PNU-159682 formation was carried out using an HPLC system consisting of a model 510 pump, a model 680 gradient controller (all from Waters), a model 7125 injector (Rheodyne), an LS-5 fluorescence spectrometer (Perkin-Elmer) and a C-R3A chromatopac integrator (Shimadzu Corp., Columbia, MD). Chromatographic conditions were as follows: column, Simmetry C_8 (4.6 × 250 mm, 5 μm; Waters); mobile phase, 10 mmol/L KH_2PO_4 (pH 5.5)/methanol/acetonitrile (45:30:25 v/v/v); flow rate, 1.5 mL/min; injection volume, 20 μL; column temperature, ambient; detection, fluorescence (excitation, 479 nm; emission, 552 nm). Under the above conditions, retention times of MMDX and PNU-159682 were 7.8 and 9.8 minutes, respectively. Quantitation of PNU-159682 was carried out by comparing peak areas to external standard calibration curves constructed daily in the range 0.03 to 1.50 nmol/0.2 mL. The calibration curves were linear over the concentration range studied ($r^2 \geq 0.98$), and the lowest value in the range represented the limit of the quantitation of the assay.

Quantitation of 3,5-Diacetyl-1,4-Dihydrolutidine. Analysis of derivatized formaldehyde (3,5-diacetyl-1,4-dihydrolutidine) was carried out using a Hewlett-Packard series 1050 HPLC system equipped with a degasser, a quaternary pump, an autosampler, and a multiple-wavelength detector (Agilent,

formerly Hewlett-Packard GmbH, Germany); chromatographic data were collected and integrated using the Hewlett-Packard ChemStation software (version A.06.03). Chromatographic conditions were as follows: column, Xterra RP_8 (4.6 × 250 mm, 5 μm; Waters); mobile phase, water/acetonitrile (80:20, v/v); flow rate, 1.3 mL/min; injection volume, 100 μL; column temperature, ambient; detection, visible absorbance at 412 nm. Under the above conditions, retention time of 3,5-diacetyl-1,4-dihydrolutidine was 6.3 minutes. Quantitation was conducted by comparing peak areas to external standard calibration curves generated from formaldehyde standards prepared daily in the range 0.4 to 40 nmol/0.4 mL. The calibration curves were linear over the concentration range studied ($r^2 \geq 0.98$), and the lowest value in the range represented the limit of the quantitation of the assay.

Cell Lines

CEM, a human lymphoblastic leukemia; Jurkat, a human T cell leukemia; DU145 a human prostatic carcinoma; and HT-29, a human colon carcinoma, were purchased from American Type Culture Collection (Rockville, MD). A2780, a human ovarian carcinoma; L1210, a murine leukemia; and MX-1, a human mammary carcinoma were from the National Cancer Institute (Frederick, MD). EM-2, a human chronic myeloid leukemia, was obtained from the German Collection of Microorganisms and Cell Cultures (DSMZ, Braunschweig, Germany). CEM cells were grown in Eagle's MEM (Life Technologies, Invitrogen Corporation, Paisley, United Kingdom). Jurkat, EM-2, and A2780 cells were maintained in RPMI 1640 (Life Technologies, Invitrogen Corporation). HT-29 cell line was maintained in Ham's F12 medium (Life Technologies, Invitrogen Corporation). DU145 and L1210 cells were grown in Dulbecco's MEM (BioWittaker, Verviers, Belgium). All culture media were supplemented with 10% (v/v) heat-inactivated FCS and 2 mmol/L glutamine (both from Life Technologies, Invitrogen Corporation); cultures were maintained at 37°C in a humidified atmosphere containing 5% CO_2. MX-1 human mammary carcinoma was maintained by serial s.c. transplantation of tumor fragments (~15-20 mg) into the flanks of 4- to 6-week-old female CD-1 athymic nude mice (from Charles River, Calco, Italy).

In vitro Cytotoxicity

The cytotoxic effects of doxorubicin, MMDX, and PNU-159682 on adherent tumor cell lines (HT-29, A2780, and DU 145) were evaluated using the sulforhodamine B assay as described by Skehan et al. (26); the effects of the drugs on the growth of nonadherent tumor cell lines (CEM, Jurkat, and EM-2) were evaluated by counting the surviving cells at the end of the treatment period with a ZM Cell Counter (Coulter Electronics, Hialeah, FL). Exponentially growing cells were seeded 24 hours before treatment and exposed to drugs for 1 hour, after which the medium was withdrawn and cells were incubated in a drug-free medium for 72 hours; control cells were not exposed to the drugs. Within each experiment, determinations were done in six replicates. IC_{70} values were then calculated from semilogarithmic concentration-response curves by linear interpolation. Data were expressed as mean ± SE of at least three independent experiments.

In vivo Tumor Models and Treatments

All procedures involving animals and their care were in conformity with institutional guidelines that comply with national and international laws and policies (European Economic Community Council Directive 86/609, OJ L 358, 1, Dec. 12, 1987; NIH Guide for the Care and Use of Laboratory Animals, NIH Publication no. 85-23, 1985).

Disseminated L1210 Leukemia. Eight-week-old inbred female CD2F1 (BALB/c × DBA/2; from Charles River) were used for evaluation of the therapeutic efficacy of PNU-159682, in comparison with that of MMDX. Disseminated neoplasia was induced by i.v. injection of 10^5 L1210 cells; 1 day later, the animals were randomly assigned to an experimental group (n = 10) and received a single i.v. injection of MMDX, PNU-159682, or saline (control group). Treatment efficacy was evaluated by comparing the median survival time in the treated and control groups, and expressed as increase in life span as follows: % increase in life span = (100 × median survival time of drug treated mice / median survival time of control mice) − 100. Statistical comparison between the groups was made using the nonparametric Mann-Whitney test (GraphPad Instat version 2.02, GraphPad Software).

Subcutaneous MX-1 Human Mammary Adenocarcinoma Xenografts. Four- to six-week-old female CD-1 athymic nude mice (from Charles River) were used for evaluation of the activity of PNU-159682 against MX-1 human mammary carcinoma xenografts. On day 0, animals (n = 14) were grafted s.c. with MX-1 tumor fragments in the right flank. Eight days later, they were randomly assigned to the drug treatment group or control group (n = 7 mice per group), and treatment was started. PNU-159682 was given i.v. (4 μg/kg) according to a q7dx3 (every 7 days for three doses) schedule; control animals received saline injections. Tumor volume was estimated from measurements done with a caliper using the formula: tumor volume (mm^3) = $D \times d^2 / 2$; where D and d are the longest and the shortest diameters, respectively. For ethical reasons, control animals were sacrificed on day 21 when the mean tumor volume in the group was ~2,500 mm^3; animals receiving drug treatment were monitored up to day 50, at which point they were sacrificed.

RESULTS

Metabolic Profile of MMDX in Human Liver Microsomes

Analysis of incubation mixtures containing [^{14}C]MMDX, NADPH, and native HLMs by reversed-phase HPLC coupled to UV and radiometric detection showed, apart from [^{14}C]MMDX, five new UV-absorbing and radioactive peaks, which were undetectable when NADPH was omitted from the mixture or when the incubation was done using heat-inactivated (boiled) microsomes; a typical radiochromatogram is shown in Fig. 1. The main peak eluting at 8 minutes corresponded to unmodified [^{14}C]MMDX, whereas the peak of the major metabolite (M5) eluted at 11.3 minutes. The retention time of this metabolite was identical to that of authentic synthetic PNU-159682, a liver microsomal metabolite of MMDX we previously identified in the rat, and chemically characterized by mass spectrometry and nuclear magnetic resonance spectroscopy (14). None of the minor metabolite peaks had a retention time

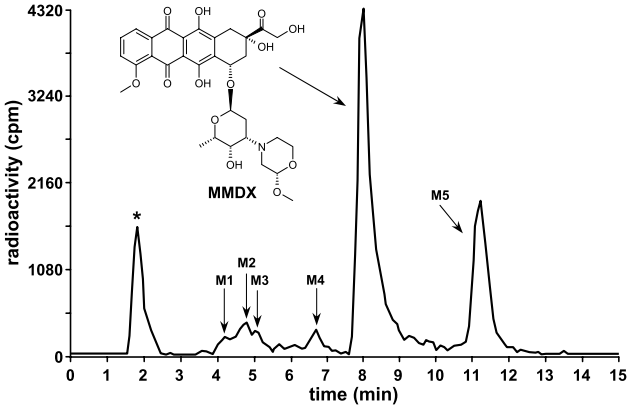

Fig. 1 Typical HPLC separation with radioactivity monitoring of MMDX and its human liver microsomal metabolites. Pooled HLMs (0.25 mg/mL) were incubated with 10 μmol/L [^{14}C]MMDX and NADPH (0.5 mmol/L) at 37°C for 30 minutes. The sample was processed and analyzed by radio-HPLC as described in Materials and Methods. The peaks marked M1 to M4 correspond to unidentified metabolites. Peak M5 corresponds to PNU-159682. The peak marked with an asterisk (*) was also present when NADPH was omitted from the incubation mixture or reaction was conducted using boiled microsomes, whereas peaks M1 to M4 and M5 were absent.

identical to that of the available authentic standard of other known metabolites of MMDX, i.e., MMDX *N*-oxide and 13-dihydro-MMDX. The identity of M5 was further supported by identical retention time, *m*/*z* of parent ion and mass spectral fragmentation pattern, as compared with the synthetic standard of PNU-159682 during analysis of reaction mixtures with LC-MS/MS. The molecular weight of the metabolite was 642, 2 a.m.u. lower than that of MMDX. The LC-MS/MS spectrum showed a major ion at *m*/*z* 228 and significant fragment ions at *m*/*z* 397, 379, 361, and 321 (Fig. 2). Formation of ions at *m*/*z* 397, 379, and 361 is in agreement with a fragmentation resulting from cleavage of the glycone moiety with subsequent loss of two molecules of water. The ions at *m*/*z* 612 and 230 in MMDX are reduced by 2 a.m.u. to 610 and 228 in PNU-159682, as they result from ions containing the glycone moiety, thus confirming that the loss of 2 a.m.u. occurs in this part of the molecule, as illustrated in Fig. 2.

Kinetics of PNU-159682 Formation in Human Liver Microsomes

Preliminary kinetic determinations showed that PNU-159682 formation from MMDX catalyzed by pooled HLMs proceeded linearly with incubation time up to at least 20 minutes and with increasing amounts of microsomal protein up to 0.5 mg/mL. The metabolite formation was then assayed under linear reaction conditions (0.25 mg of microsomal protein/mL; 10 minutes incubation) over a substrate concentration range of 1 to 50 μmol/L. The Eadie-Hofstee plot of data (rate of PNU-159682 formation versus rate of PNU-159682 formation/MMDX concentration) was linear (data not shown), suggesting that a single microsomal enzyme or multiple enzymes with similar apparent K_m values can catalyze conversion of MMDX to PNU-159682. The K_m and V_{max} values were 16.20 ± 1.18 μmol/L and 2.29 ± 0.07 nmol/minute/mg protein, respectively (mean ± SE of the parameter estimate). Based on these findings, further analyses of the conversion of MMDX to PNU-159682 by HLMs were carried out by incubating MMDX at 20 μmol/L (i.e., at a concentration close to the K_m value for this reaction) with 0.25 mg/mL microsomal protein for 10 minutes at 37°C.

Identification of CYP3A4 as the Enzyme Responsible for Conversion of MMDX into PNU-159682 in Human Liver Microsomes

Several approaches were used to identify the enzyme(s) responsible for the biotransformation of MMDX into its major human liver microsomal metabolite. In a first set of experiments, the rates of PNU-159682 formation were evaluated in fully characterized liver microsomes from 10 subjects. Results (Fig. 3*A*) indicated a 14-fold variability among individuals because rates of metabolite formation ranged between 0.28 ± 0.02 and 3.96 ± 0.11 nmol/minute/mg protein (mean ± SE of three independent experiments), whereas the mean rate (± SE) was 1.64 ± 0.39 nmol/minute/mg protein. The reaction velocity data were then analyzed for correlation with total CYP content and several CYP form-selective activities evaluated in the same microsomal samples. Highly significant correlations were noted between the rate of PNU-159682 formation and three markers of CYP3A4/5 catalytic activity (Fig. 3*B*, *C*, and *D*), that is the rate of testosterone 6β-hydroxylation (r^2 = 0.9909; P < 0.0001), the rate of nifedipine oxidation (r^2 = 0.9520; P < 0.0001) and the rate of erythromycin *N*-demethylation (r^2 = 0.9542; P < 0.0001). The sample-to-sample variation in the rate of PNU-159682 formation also correlated significantly with total CYP content (r^2 0.8509; P < 0.0001; data not shown). Conversely,

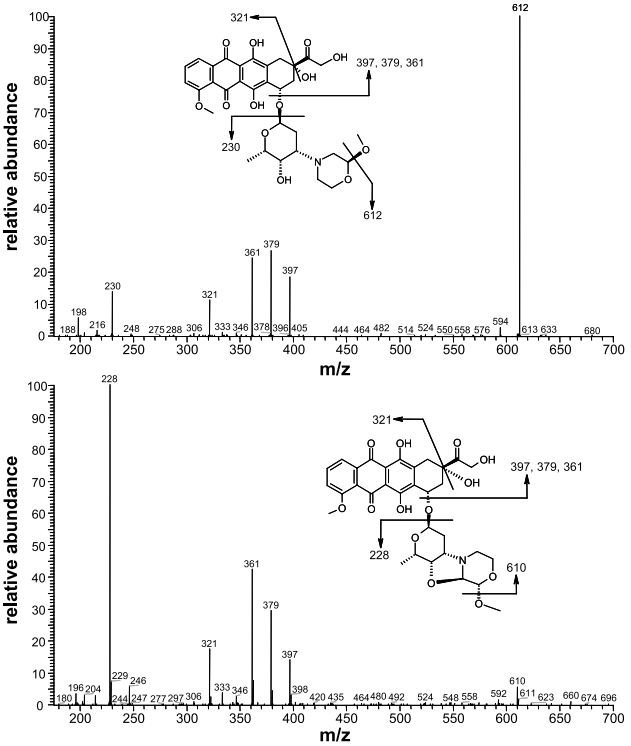

Fig. 2 Tandem mass spectra collected from the peaks of MMDX (*top*) and PNU-159682 (*bottom*). Inset, proposed fragmentation.

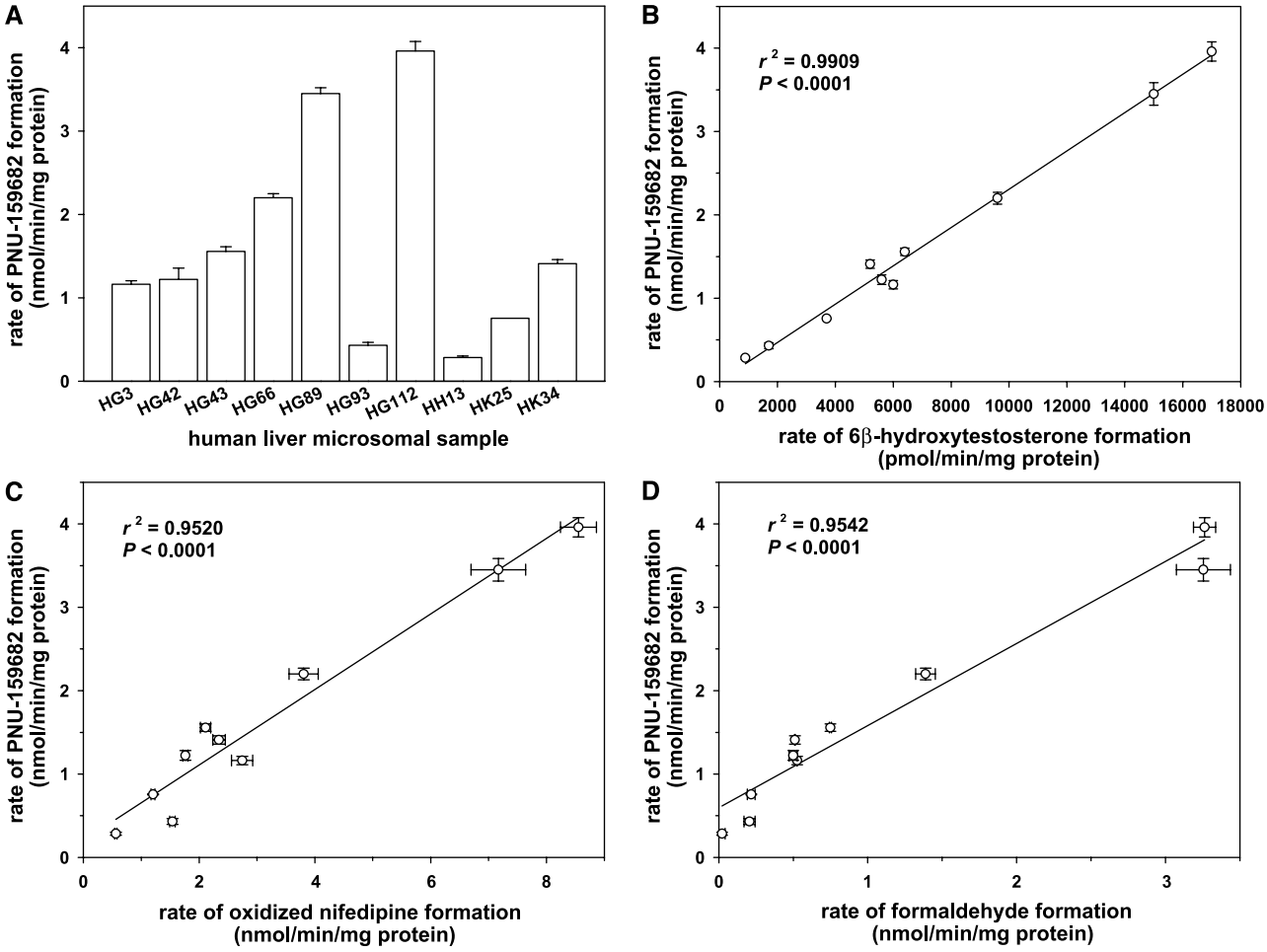

Fig. 3 Variability in the rate of PNU-159682 formation in a panel of HLMs and correlation analyses. *A,* MMDX (20 μmol/L) was incubated with 10 human liver microsomal samples (0.25 mg/mL) in the presence of NADPH (0.5 mmol/L) at 37°C for 10 minutes. Incubation mixtures were then processed and analyzed for PNU-159682 content by HPLC as described in Materials and Methods. Columns, mean; bars, ± SE of three independent experiments. *B, C,* and *D,* correlation between the rate of PNU-159682 formation and CYP3A-mediated activities. The rates of 6β-hydroxytestosterone formation were obtained from the individual HLMs data sheet published by BD Gentest. Nifedipine oxidase and erythromycin *N*-demethylase activities of each liver microsomal sample were assayed as described in Materials and Methods. The rates of formation of PNU-159682, oxidized nifedipine, and formaldehyde are shown as mean ± SE of three independent experiments carried out in duplicate. The solid lines represent the linear regression equations.

no correlation was observed between the rate of PNU-159682 formation and the rates of phenacetin *O*-deethylation (CYP1A2), coumarin 7-hydroxylation (CYP2A6), *S*-mephenytoin *N*-demethylation (CYP2B6), paclitaxel 6α-hydroxylation (CYP2C8), diclofenac 4′-hydroxylation (CYP2C9), *S*-mephenytoin 4′-hydroxylation (CYP2C19), bufuralol 1′-hydroxylation (CYP2D6), chlorzoxazone 6-hydroxylation (CYP2E1), and lauric acid 12-hydroxylation (CYP4A; r^2 range from 0.0001 to 0.1234; all $P > 0.37$).

Subsequent experiments examined the effects of CYP form-selective chemical inhibitors and CYP form-specific inhibitory MAbs on MMDX metabolism to PNU-159682 by HLMs. Among the chemicals tested, only ketoconazole (1 μmol/L) and troleandomycin (100 μmol/L), both selective inhibitors of CYP3A enzymes in HLMs (22, 25), effectively decreased the rate of PNU-159682 formation (81.4% and 94.7% reduction, respectively; Fig. 4*A*). Sulfaphenazole (20 μmol/L, CYP2C9-selective; ref. 22), quinidine (5 μmol/L, CYP2D6-selective; ref. 22) and diethyldithiocarbamate (25 μmol/L, CYP2A6/2E1-selective; ref. 24) were relatively weak inhibitors of metabolite formation (≤10% reduction of metabolite formation rate), whereas 7,8-benzoflavone (1 μmol/L), a selective inhibitor of CYP1A2 (22, 23) and a stimulator of some reactions supported by CYP3A4 (27, 28), gave a 12.8% increase of the rate of PNU-159682 formation (Fig. 4*A*); a higher concentration of this flavonoid (30 μmol/L) caused a substantial (2.5-fold) increase of the reaction rate (not shown). Immunoinhibition studies showed a concentration-dependent inhibitory effect of anti-CYP3A4/5 MAb on formation of PNU-159682; at a concentration of 700 μg ascites protein/mL this MAb preparation yielded 83.2% reduction of the rate of metabolite formation (Fig. 4*B*). By contrast, anti-CYP1A2, anti-CYP2B6, anti-CYP2C8, anti-CYP2C9, anti-CYP2C19, and anti-CYP2D6 MAbs, at their recommended inhibitory

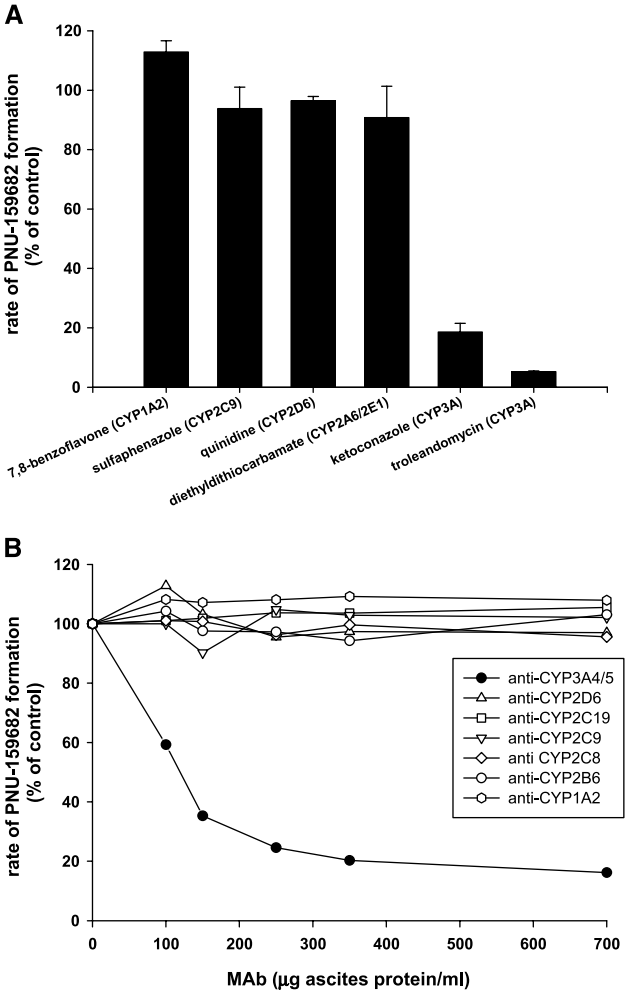

Fig. 4 Effects of CYP form-selective inhibitors (*A*) and anti-CYP MAbs (*B*) on the conversion of MMDX to PNU-159682 by HLMs. *A,* all incubations were carried out in the absence (control) or presence of appropriate concentrations of chemical inhibitors, as described in Materials and Methods, at 37°C for 10 minutes, using pooled HLMs (0.25 mg/mL), MMDX (20 µmol/L), and NADPH (0.5 mmol/L). Values represent percentage of control activity, and are the mean ± SE of three independent experiments; *B,* pooled HLMs (20 pmol of total CYP), preincubated in the absence or presence of increasing amounts of MAb at 37°C for 5 minutes, were incubated with MMDX (20 µmol/L) and NADPH (0.5 mmol/L) at 37°C for 10 minutes. Values represent percentage of control activity determined in the absence of MAb, and are the mean of duplicate determinations. PNU-159682 formation was analyzed by HPLC as described in Materials and Methods.

concentrations (15–19), had no significant effects on metabolite formation (Fig. 4*B*).

A last set of reaction phenotyping experiments examined the catalytic competence of microsomal preparations containing individual recombinant human CYP enzymes, in the conversion of MMDX to PNU-159682. Although 20 µmol/L MMDX was metabolized to PNU-159682 by cDNA-expressed CYP3A4 (46 pmol PNU-159682 formed/60 minute/pmol CYP), microsomes containing CYP1A2, CYP2A6, CYP2B6, CYP2C8, CYP2C9*1, CYP2C19, CYP2D6*1, CYP2E1, or CYP3A5 did not produce any detectable amount of the metabolite.

In vitro Cytotoxicity and *In vivo* Antitumor Activity of PNU-159682

The cytotoxicity of PNU-159682 toward six cultured human tumor cell lines of different histotypes were compared with that of MMDX and doxorubicin. Results are summarized in Table 1. IC_{70} values of PNU-159682 were in the subnanomolar range (0.07-0.58 nmol/L) and noticeably lower than that recorded for both MMDX and doxorubicin; PNU-159682 was 2,360- to 790-fold and 6,420- to 2,100-fold more potent than MMDX and doxorubicin, respectively (Table 1).

An evaluation of the *in vivo* antitumor activity of PNU-159682, in comparison with that of MMDX, was then conducted in mice bearing disseminated murine L1210 leukemia. Preliminary toxicity dose-finding studies showed that 15 µg/kg i.v. was the single-dose maximum tolerated dose of PNU-159682. The antitumor effect observed after administration of this dose of PNU-159682 (increase in life span = 29%; $P < 0.0001$ versus control) was comparable ($P = 0.31$) to that afforded by 90 µg/kg MMDX (increase in life span = 36%; $P < 0.0001$ versus control), which represents the optimal dose of MMDX using a single-dose schedule i.v. (1, 9).

A further experiment estimated the antitumor activity of PNU-159682 in athymic nude mice bearing MX-1 human mammary carcinoma xenografts. This tumor is refractory to doxorubicin treatment (1, 29) but highly sensitive to MMDX, with most treated animals showing complete response after repeated i.v. or p.o. administration (1). Drug treatment began on day 8 after tumor implantation and consisted of 4 µg/kg PNU-159682 i.v. every 7 days for three times (q7dx3 schedule). As shown in Fig. 5, PNU-159682 was remarkably active against MX-1 xenografts causing tumor regression in all treated animals. Complete tumor response (i.e., no palpable tumor) was observed in four out of seven animals. Nevertheless, as the maximum tolerated dose of PNU-159682 with a q7dx3 schedule was not determined, the complete response rate achievable in this tumor model may be even greater with schedule optimization.

Table 1 IC_{70} values (nmol/L) of doxorubicin, MMDX, and PNU-159682 in a panel of human tumor cell lines

	HT-29	A2780	DU145	EM-2	Jurkat	CEM
Doxorubicin	1,279 ± 324*	1,717 ± 581	443 ± 26	521 ± 153	181 ± 29	391 ± 38
MMDX	578 ± 137	468 ± 45	193 ± 28	191 ± 19	68 ± 12	131 ± 9
PNU-159682	0.577 ± 0.140	0.39 ± 0.0016	0.128 ± 0.030	0.081 ± 0.003	0.086 ± 0.016	0.075 ± 0.020

NOTE. Each tumor cell line was exposed to the drugs for 1 hour and then cultured in drug-free medium for 72 hours. Growth inhibition assays were done as described in Materials and Methods.

*Each IC_{70} value (nmol/L) is the mean ± SE of at least three independent experiments, each consisting of six replicates.

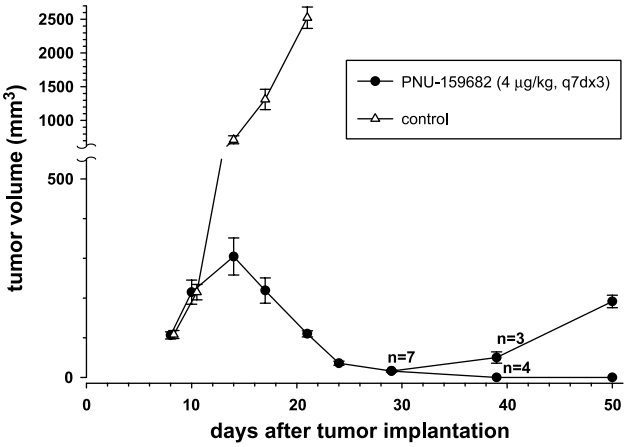

Fig. 5 Therapeutic response of MX-1 human mammary carcinoma xenografts to PNU-159682. MX-1 tumor fragments were implanted s.c. into the right flank of athymic mice (day 0; $n = 14$). Eight days after tumor implantation, when tumor volume was 107.0 ± 6.5 mm^3 (mean ± SE), seven animals were randomly assigned to the treatment group and drug treatment was started. PNU-159682 was given i.v. every 7 days for three times (q7dx3 schedule). Tumor volumes were evaluated as described in Materials and Methods until the animals were sacrificed. Points, mean tumor volume (mm^3; $n = 7$ animals per group); bars, ± SE. From day 39, four out of seven mice receiving PNU-159682 exhibited complete tumor regression (i.e., showed no palpable tumor).

DISCUSSION

The study described here shows that CYP3A4 is the predominant, if not the only, human CYP enzyme responsible for formation of PNU-159682, i.e., the major liver microsomal metabolite and bioactivation product of MMDX. The conclusion of CYP3A4-selective catalysis is derived from the results of an integrated *in vitro* approach (30, 31) based on: (*a*) analysis of the possible correlation between the rates of PNU-159682 formation and several CYP form-selective activities in a panel of HLMs from 10 subjects, (*b*) evaluation of the effects of CYP form-selective chemical inhibitors and MAbs specific and inhibitory to different human hepatic CYPs, on MMDX conversion to PNU-159682 by pooled HLMs, and (*c*) evaluation of the intrinsic ability of individual recombinant human CYP enzymes to catalyze formation of the metabolite. Correlation studies showed that the rate of PNU-159682 formation was highly significantly correlated with three different CYP3A-mediated activities (Fig. 3*B*, *C* and *D*) but did not correlate with marker activities of nine other CYPs in the bank of HLMs. Chemical and immunochemical inhibition of liver microsomal CYP3A resulted in marked (>80%) inhibition of MMDX metabolism to PNU-159682 (Fig. 4). On the other hand, inhibition (by chemicals and/or MAbs) of other CYP enzymes responsible for human drug metabolism (i.e., CYP1A2, CYP2A6, CYP2B6, CYP2C8, CYP2C9, CYP2C19, CYP2D6, and CYP2E1) did not result in any significant reduction of the rate of PNU-159682 formation. Further corroborating the role of CYP3A4 in this biotransformation, formation of PNU-159682 was catalyzed only by cDNA-expressed CYP3A4 but not by any of the other nine recombinant CYP enzymes examined, including CYP3A5. Moreover, consistent with the involvement of a single CYP form, conversion of MMDX to PNU-159682 catalyzed by HLMs conformed to single-enzyme Michaelis-Menten kinetics (not shown).

Further *in vitro* experiments aimed at obtaining information about the cytotoxicity of PNU-159682 toward human tumor cell lines of different histotype confirmed the much higher potency of this compound, compared with MMDX and doxorubicin (Table 1). Moreover, PNU-159682 showed moderate activity against disseminated murine L1210 leukemia in CD2F1 mice (increase in life span = 29%; $P < 0.0001$ versus control) and remarkable effectiveness toward MX-1 human mammary tumor xenografts in nude mice (Fig. 5); the profile of *in vivo* antitumor efficacy of PNU-159682 seems therefore to mimic that of its parent compound, MMDX (1, 9). This is not surprising because based on its extremely higher potency compared with MMDX, and requirement of catalysis by CYP3A for its formation, PNU-159682 plays a role in the *in vivo* antitumor activity and host toxicity of MMDX (9). A role of metabolism in the activity of MMDX *in vivo* is also suggested by the lack of correlation between drug plasma area under the curve and hematologic and nonhematologic toxicity observed during phase I and II clinical trials (32, 33). Ongoing studies aimed at exploring the molecular mechanism of action of PNU-159682 indicate that it has different effects on cell cycle progression and different DNA-interacting properties, compared with both MMDX and doxorubicin (34). Moreover, further recent data suggest that PNU-159682 retains its activity against tumor cell lines with different mechanisms of resistance to classical anticancer agents, including *MDR-1* gene overexpression, reduced topoisomerase II activity, and mutations in the *topoisomerase I* gene, these latter genetic alterations conferring resistance *in vitro* to the parent drug, MMDX (35).

The conclusion that CYP3A4 is responsible for the oxidative bioactivation of MMDX in humans is important considering that this CYP contributes, at least partially, to the metabolism of ~50% of the drugs for which the enzymes responsible for their metabolism have been identified to date, including several anticancer agents (36). CYP3A4 is universally expressed in adult human liver accounting for, on average, 29% of the total hepatic CYP (37) and relatively high levels of the protein (~50% of hepatic levels) are also present in the small intestine, playing a significant role in the first pass metabolism of various drugs (38). Furthermore, there is high variability in the constitutive levels and activity of hepatic and intestinal CYP3A4 between individuals, which has been reported to range by at least 30-fold (38). It has been recently concluded that genetic factors are of great importance for the interindividual variability in constitutive levels of CYP3A4, accounting for 70% to 90% of the variation, although the underlying mechanisms are still unknown (39). In addition, it is well known that such differences in constitutive CYP3A4 activity can be increased significantly by induction and inhibition of the enzyme by several common drugs, which could therefore cause clinically important variation in MMDX toxicity and efficacy, as previously shown for several other drugs (40). With regard to this, although induction of murine hepatic CYP3A did not cause any significant alteration of the activity of MMDX *in vivo*, administration of the selective CYP3A inhibitor troleandomycin, markedly decreased the therapeutic effects of the drug in tumor-bearing mice (9). Administration of potent inhibitors of CYP3A4 activity such as azole antifungals (e.g., ketoconazole and itraconazole) and some macrolide antibiotics (e.g., erythromycin and troleandomycin) should

therefore be avoided during chemotherapy with MMDX, to reduce the risk of a therapeutic failure due to inefficient oxidative bioactivation of the drug. Monitoring of plasma levels of PNU-159682 during therapy with MMDX should help to individuate the optimum therapeutic concentrations of the metabolite, and allow adjustment of drug doses which will ideally minimize toxicity and maximize successful treatment with MMDX. *In vitro* drug interaction studies based on evaluation of the inhibitory effects of MMDX and PNU-159682 on hepatic CYP form-specific activities are in progress at our laboratory, to determine whether MMDX may potentially affect the CYP-mediated metabolism of concurrently given drugs.

Some *CYP* genes including *CYP3A4* have been found to be expressed in several human neoplasms, including hepatocellular carcinomas (41), which are poorly responsive to chemotherapy (42). Furthermore, it has been recently shown that microsomes from colorectal cancer samples have the ability to convert paclitaxel to a less cytotoxic metabolite, 3′-*p*-hydroxypaclitaxel (43); this metabolic reaction is known to be selectively catalyzed by CYP3A4 (44). Besides paclitaxel, CYP3A4 has been shown to be involved in the metabolic inactivation of several other anticancer agents such as docetaxel, *Vinca* alkaloids, and irinotecan (44–46). It is conceivable that expression of CYP3A4 by tumor cells *in vivo* may negatively modulate their sensitivity to these agents as it has recently been shown *in vitro* for paclitaxel, vincristine, and vinblastine, using stably transfected cell lines expressing CYP3A4 (45, 47). By contrast, patients with tumors expressing functional CYP3A4 may benefit from treatment with MMDX due to intratumoral conversion of the drug into a highly potent cytotoxin, PNU-159682.

In conclusion, our findings point to a determinant role of human CYP3A4 in the conversion of MMDX to its highly cytotoxic metabolite, PNU-159682, and suggest that further studies are needed to appreciate the role of intratumoral activation in the patients' response to the drug.

ACKNOWLEDGMENTS

We thank D.J. Waxman, I. Poggesi, and R. Padrini for critically reading the manuscript; H.V. Gelboin for providing us with inhibitory anti-CYP monoclonal antibodies; K.W. Krausz for advice on their use; R.O. Strobl for assistance in preparing the manuscript; and P. Favero for competent technical assistance.

REFERENCES

1. Ripamonti M, Pezzoni G, Pesenti E, et al. *In vivo* anti-tumour activity of FCE 23762, a methoxymorpholinyl derivative of doxorubicin active on doxorubicin-resistant tumour cells. Br J Cancer 1992; 65:703–7.

2. Bakker M, Renes J, Groenhuijzen A, et al. Mechanisms for high methoxymorpholino doxorubicin cytotoxicity in doxorubicin-resistant tumor cell lines. Int J Cancer 1997;73:362–6.

3. Mariani M, Capolongo L, Suarato A, et al. Growth-inhibitory properties of novel anthracyclines in human leukemic cell lines expressing either Pgp-MDR or at-MDR. Invest New Drugs 1994;12:93–7.

4. Danesi R, Agen C, Grandi M, Nardini V, Bevilacqua G, Del Tacca M. 3′-Deamino-3′-(2-methoxy-4-morpholinyl)-doxorubicin (FCE 23762): a new anthracycline derivative with enhanced cytotoxicity and reduced cardiotoxicity. Eur J Cancer 1993;11:1560–5.

5. Sun Y, et al. Efficacy of nemorubicin (MMDX) administered with iodinated oil via hepatic artery (IHA) to patients with unresectable primary hepatocellular carcinoma (HCC): phase II trial. Abstract presented to the 16th EORTC-NCI-AACR Symposium on Molecular Targets and Cancer Therapeutics; 28 September-1 October 2004; Geneva, Switzerland .

6. Vasey PA, Bissett D, Strolin-Benedetti M, et al. Phase I clinical and pharmacokinetic study of 3′-deamino-3′-(2-methoxy-4-morpholinyl)doxorubicin (FCE 23762). Cancer Res 1995;55:2090–6.

7. Quintieri L, Rosato A, Amboldi N, et al. Delivery of methoxymorpholinyl doxorubicin by interleukin 2-activated NK cells: effect in mice bearing hepatic metastases. Br J Cancer 1999;79:1067–73.

8. Lau DH, Duran GE, Lewis AD, Sikic BI. Metabolic conversion of methoxymorpholinyl doxorubicin: from a DNA strand breaker to a DNA cross-linker. Br J Cancer 1994;70:79–84.

9. Quintieri L, Rosato A, Napoli E, et al. *In vivo* antitumor activity and host toxicity of methoxymorpholinyl doxorubicin: role of cytochrome *P*450 3A. Cancer Res 2000;60:3232–8.

10. Baldwin A, Huang Z, Jounaidi Y, Waxman DJ. Identification of novel enzyme-prodrug combinations for use in cytochrome *P*450-based gene therapy for cancer. Arch Biochem Biophys 2003;409:197–206.

11. Breda M, Strolin-Benedetti M, Battaglia R, et al. Species-differences in disposition and reductive metabolism of methoxymorpholinodoxorubicin (PNU 152243), a new potential anticancer agent. Pharmacol Res 2000;41:239–48.

12. Schott B, Robert J. Comparative activity of anthracycline 13-dihydrometabolites against rat glioblastoma cells in culture. Biochem Pharmacol 1989;38:4069–74.

13. Sessa C, Zucchetti M, Ghielmini M, et al. Phase I clinical and pharmacological study of oral methoxymorpholinyl doxorubicin (PNU 152243). Cancer Chemother Pharmacol 1999;44:403–10.

14. Suarato A, Caruso M, Geroni C, Capolongo L, Pennella G. From anthracyclines to alkycyclines. In: Book of Abstracts of the 217th American Chemical Society National Meeting, Anaheim, CA, March 21–25 1999. Abstr. CARB–071.

15. Gelboin HV, Krausz KW, Goldfarb I, et al. Inhibitory and non-inhibitory monoclonal antibodies to human cytochrome *P*450 3A3/4. Biochem Pharmacol 1995;50:1841–50.

16. Krausz KW, Yang TJ, Gonzalez FJ, Shou M, Gelboin HV. Inhibitory monoclonal antibodies to human cytochrome *P*450 2D6. Biochem Pharmacol 1997;54:15–7.

17. Yang TJ, Krausz KW, Shou M, et al. Inhibitory monoclonal antibody to human cytochrome *P*450 2B6. Biochem Pharmacol 1998;55:1633–40.

18. Yang TJ, Sai Y, Krausz KW, Gonzalez FJ, Gelboin HV. Inhibitory monoclonal antibodies to human cytochrome *P*450 1A2: analysis of phenacetin *O*-deethylation in human liver. Pharmacogenetics 1998; 8:375–82.

19. Krausz KW, Goldfarb I, Buters JT, Yang TJ, Gonzalez FJ, Gelboin HV. Monoclonal antibodies specific and inhibitory to human cytochromes P450 2C8, 2C9, and 2C19. Drug Metab Dispos 2001;29: 1410–23.

20. Guengerich FP, Martin MV, Beaune PH, Kremers P, Wolff T, Waxman DJ. Characterization of rat and human liver microsomal cytochrome P-450 forms involved in nifedipine oxidation, a prototype for genetic polymorphism in oxidative drug metabolism. J Biol Chem 1986;261:5051–60.

21. Jones SB, Terry CM, Lister TE, Johnson DC. Determination of submicromolar concentrations of formaldehyde by liquid chromatography. Anal Chem 1999;71:4030–3.

22. Newton DJ, Wang RW, Lu AY. Cytochrome *P*450 inhibitors. Evaluation of specificities in the *in vitro* metabolism of therapeutic agents by human liver microsomes. Drug Metab Dispos 1995;23: 154–8.

23. Ono S, Hatanaka T, Hotta H, Satoh T, Gonzalez FJ, Tsutsui M. Specificity of substrate and inhibitor probes for cytochrome *P*450s: evaluation of *in vitro* metabolism using cDNA-expressed human P450s and human liver microsomes. Xenobiotica 1996;26: 681–93.

24. Hickman D, Wang JP, Wang Y, Unadkat JD. Evaluation of the selectivity of *In vitro* probes and suitability of organic solvents for the

measurement of human cytochrome *P*450 monooxygenase activities. Drug Metab Dispos 1998;26:207–15.

25. Bourrie M, Meunier V, Berger Y, Fabre G. Cytochrome *P*450 isoform inhibitors as a tool for the investigation of metabolic reactions catalyzed by human liver microsomes. J Pharmacol Exp Ther 1996;277:321–32.

26. Skehan P, Storeng R, Scudiero D, et al. New colorimetric cytotoxicity assay for anticancer-drug screening. J Natl Cancer Inst 1990;82:1107–12.

27. Shou M, Grogan J, Mancewicz JA, et al. Activation of CYP3A4: evidence for the simultaneous binding of two substrates in a cytochrome *P*450 active site. Biochemistry 1994;33:6450–5.

28. Ueng YF, Kuwabara T, Chun YJ, Guengerich FP. Cooperativity in oxidations catalyzed by cytochrome *P*450 3A4. Biochemistry 1997;36:370–81.

29. Pratesi G, Polizzi D, Perego P, Dal Bo L, Zunino F. Bcl-2 phosphorylation in a human breast carcinoma xenograft: a common event in response to effective DNA-damaging drugs. Biochem Pharmacol 2000;60:77–82.

30. Rodrigues AD. Use of *in vitro* human metabolism studies in drug development. An industrial perspective. Biochem Pharmacol 1994;48:2147–56.

31. Lu AY, Wang RW, Lin JH. Cytochrome *P*450 *in vitro* reaction phenotyping: a re-evaluation of approaches used for P450 isoform identification. Drug Metab Dispos 2003;31:345–50.

32. Bakker M, Droz JP, Hanauske AR, et al. Broad phase II and pharmacokinetic study of methoxy-morpholino doxorubicin (FCE 23762-MMRDX) in non-small-cell lung cancer, renal cancer and other solid tumour patients. Br J Cancer 1998;77:139–46.

33. Fokkema E, Verweij J, van Oosterom AT, et al. A prolonged methoxymorpholino doxorubicin (PNU-152243 or MMRDX) infusion schedule in patients with solid tumours: a phase 1 and pharmacokinetic study. Br J Cancer 2000;82:767–71.

34. Quintieri L, Lobo Antunes J, Saggioro D, et al. *In vitro* cytotoxicity, cell cycle effects and DNA-binding properties of PNU-159682. Proc Amer Assoc Cancer Res (2nd ed.) 2003;44:925.

35. Geroni C, Marsiglio A, Amboldi N, Ballinari D, Saggioro D, Quintieri L. Sensitivity of different drug-resistant cell lines to nemorubicin and its metabolites. J Chemother 2004;16(Suppl.1):169.

36. Guengerich FP. Cytochrome P-450 3A4: regulation and role in drug metabolism. Annu Rev Pharmacol Toxicol 1999;39:1–17.

37. Shimada T, Yamazaki H, Mimura M, Inui Y, Guengerich FP. Interindividual variations in human liver cytochrome P-450 enzymes involved in the oxidation of drugs, carcinogens and toxic chemicals: studies with liver microsomes of 30 Japanese and 30 Caucasians. J Pharmacol Exp Ther 1994;270:414–23.

38. Paine MF, Khalighi M, Fisher JM, et al. Characterization of interintestinal and intraintestinal variations in human CYP3A-dependent metabolism. J Pharmacol Exp Ther 1997;283:1552–62.

39. Ozdemir V, Kalowa W, Tang BK, et al. Evaluation of the genetic component of variability in CYP3A4 activity: a repeated drug administration method. Pharmacogenetics 2000;10:373–88.

40. Lin JH, Lu AY. Inhibition and induction of cytochrome *P*450 and the clinical implications. Clin Pharmacokinet 1998;35:361–90.

41. Patterson LH, Murray GI. Tumour cytochrome *P*450 and drug activation. Curr Pharm Des 2002;8:1335–47.

42. Schwartz JD, Schwartz M, Mandeli J, Sung M. Neoadjuvant and adjuvant therapy for resectable hepatocellular carcinoma: review of the randomised clinical trials. Lancet Oncol 2002;3:593–603.

43. Martinez C, Garcia-Martin E, Pizarro RM, Garcia-Gamito FJ, Agundez JA. Expression of paclitaxel-inactivating CYP3A activity in human colorectal cancer: implications for drug therapy. Br J Cancer 2002;87:681–6.

44. Cresteil T, Monsarrat B, Dubois J, Sonnier M, Alvinerie P, Gueritte F. Regioselective metabolism of taxoids by human CYP3A4 and 2C8: structure-activity relationship. Drug Metab Dispos 2002;30:438–45.

45. Yao D, Ding S, Burchell B, Wolf CR, Friedberg T. Detoxication of *Vinca* alkaloids by human P450 CYP3A4-mediated metabolism: implications for the development of drug resistance. J Pharmacol Exp Ther 2000;294:387–95.

46. Mathijssen RH, van Alphen RJ, Verweij J, et al. Clinical pharmacokinetics and metabolism of irinotecan (CPT-11). Clin Cancer Res 2001;7:2182–94.

47. Philip PA, Ali-Sadat S, Doehmer J, et al. Use of V79 cells with stably transfected cytochrome *P*450 cDNAs in studying the metabolism and effects of cytotoxic drugs. Cancer Chemother Pharmacol 1999;43:59–67.